

Effect of SiC content on the processing, compaction behavior, and properties of Al6061/SiC/Gr hybrid composites

Soheil Mahdavi · Farshad Akhlaghi

Received: 5 June 2010 / Accepted: 24 September 2010 / Published online: 14 October 2010
© Springer Science+Business Media, LLC 2010

Abstract Aluminum matrix composites reinforced with SiC and graphite (Gr) particles are a unique class of advanced engineered materials that have been developed to use in tribological applications. The conventional techniques for producing these composites have some drawbacks. In this study, a new method, namely In situ Powder Metallurgy (IPM), is applied for the preparation of Al6061/SiC/Gr hybrid composites. In this method, the stir casting and the powder metallurgy synthesizing processes are combined into an integrated net shape forming process. 0–40 vol.% of SiC particles with an average size of 19 µm, along with 9 vol.% of uncoated Gr particles, were introduced to the molten 6061 aluminum alloy. Then, the slurries were stirred in a specified time–temperature regime resulting in mixtures of the SiC, Gr, and aluminum powder particles. The powder mixtures were cold pressed in six different pressures (between 250 and 750 MPa) and sintered. Finally, the produced composites were heat treated and their hardness and wear properties were investigated. Homogenous distribution of the SiC and Gr particles within the powder mixtures and the hybrid composites is clear from the SEM images. The results also show that the SiC particles decrease the compressibility of the hybrid powders and improve the hardness of composites. The best wear resistance is achieved in the hybrid composite containing 20 vol.% SiC particles.

Introduction

Particulate-reinforced aluminum matrix composites have gained extensive applications in automotive and aerospace industries due to their specific characteristics. These include low density, high specific strength and stiffness, good fatigue properties, dimensional stability at high temperatures, and acceptable tribological properties [1–12]. Among these materials, hybrid composites reinforced with SiC and graphite (Gr) particles have attracted considerable attention due to their high wear resistance combined with a low friction coefficient [11–14]. The specimen-die wall friction and the friction between particles play a critical role in the compaction process and may result in non-uniform packing densities within samples [15–17]. Adding a certain amount of solid lubricant to the powder mixture can decrease the density gradient and increase the density of green compacts by promoting more uniform pressure transmission [16–18]. Gr is frequently used as the solid lubricant, but it deteriorates the mechanical properties of composites. The presence of hard SiC particles improves the hardness and the strength of Al/SiC/Gr hybrid composites, and compensates for the weakening effects of Gr [10, 13, 19].

The main problem of hybrid composites is associated with their fabrication processes [14]. The stir casting is one of the most important liquid phase methods for processing of metal matrix composites. Poor wettability of reinforcing particles by liquid metal, and density differences between the matrix alloy and these particles result in non-uniform distribution of the reinforcement phase within the matrix alloy [7–9, 14, 20]. Moreover, the segregation of particles due to pushing effects during solidification, and formation of brittle compounds and porosity at the ceramic/matrix interface cause deterioration of the mechanical and tribological properties of the composites [6, 7, 14, 21]. Among

S. Mahdavi (✉) · F. Akhlaghi
School of Metallurgy and Materials Engineering,
College of Engineering, University of Tehran,
P.O. Box 11155-4563, Tehran, Iran
e-mail: mahdavis@ut.ac.ir

F. Akhlaghi
e-mail: fakhlagh@ut.ac.ir

the solid-state methods, powder metallurgy (P/M) is an important processing technique for metal matrix composites. The need for a relatively long mixing time to achieve a uniform distribution of ceramic particles within the aluminum powders, the re-distribution of the particles during pressing, and high processing costs are some of the drawbacks of this method [19, 20, 22, 23]. The In situ Powder Metallurgy (IPM) method is a new processing technique for metal matrix composites. In this technique, the non-wetting ceramic particles are added to the molten alloy. Then, the mixture is stirred in a specified time–temperature regime, resulting in a mixture of aluminum droplets and ceramic particles. This blend is cooled in air and the resultant mixture of aluminum and ceramic particles is consolidated to produce the final component. In this method, there are no typical limitations of the stir casting and the P/M methods. Producing dense (pore-free) aluminum powders and low processing costs are some of the other advantages of this method [20, 24–27].

Cold pressing of powder mixtures is widely used in industry, because of simplicity and high efficiency [28]. It also plays an important role in mechanical properties and dimensional tolerances of final components. The compressibility of composite powders is considerably lower than that of the unreinforced alloy. Hard-reinforcing particles complicate the compaction behavior of powder mixtures [23, 29]. In addition, the type, amount, size, and geometry (shape) are important factors for achieving the optimum combination of properties [23, 30, 31]. Moreover, amount of the applied pressure, particles size ratio in the powder mixtures, and temperature are also effective on the strength of green compacts. Hence, optimizing of these parameters has been considered by several researchers [22, 23, 28]. This study investigates applicability of IPM method for processing of the Al6061/SiC/Gr hybrid composites, effect of SiC content on the compressibility, sintering, hardness, aging behavior, and finally, tribological behavior of the hybrid composites.

Experimental procedures

Al 6061 with nominal chemical composition as given in Table 1 was used as the matrix alloy. SiC particles with average size of 19 μm together with flake Gr particles with average size of 75 μm were also used as the reinforcing particles. The size distribution of the SiC and Gr particles

Table 1 Chemical composition (wt%) of Al 6061 alloy

Mg	Si	Fe	Cu	Cr	Al
1.12	0.64	0.48	0.33	0.04	Remaining

was quantified using a laser particle size analyzer (Cilas 1064). The results are shown in Fig. 1. The SEM micrographs of these powders are shown in Fig. 2. For preparation of each powder mixture, the appropriate weights of Al ingot, SiC powders, and uncoated Gr particles were charged in a clay-bonded Gr crucible. Given density values for Al, SiC, and Gr (2.7, 3.2, and 2.2 g/cm³), the crucible charge was determined to obtain the following five different powder mixtures: 0, 10, 20, 30, and 40 vol.% of SiC particles all having 9 vol.% Gr. The crucible was heated in a resistance furnace and after melting the aluminum, the mixture was stirred at 1400 rpm for 8 min using a spiral-shaped Gr stirrer at a constant temperature of 710 °C. During stirring the mixture, molten aluminum alloy was disintegrated to droplets due to the non-wettability of SiC and Gr particles with molten aluminum alloy, and the shear forces induced by the impeller. Figure 3 schematically shows the powder mixture condition in the different steps of the stirring process. The mixture was evacuated from the crucible onto a steel flat plate and the alloy was allowed to solidify at ambient temperature and atmosphere. This procedure was performed using different volume fractions of the SiC particles. Coarse alumina particles (>710 μm) were also used to produce the base alloy powder particles using IPM method. After producing the powder mixtures of the aluminum alloy and alumina particles at the same condition with those previously produced by the SiC and

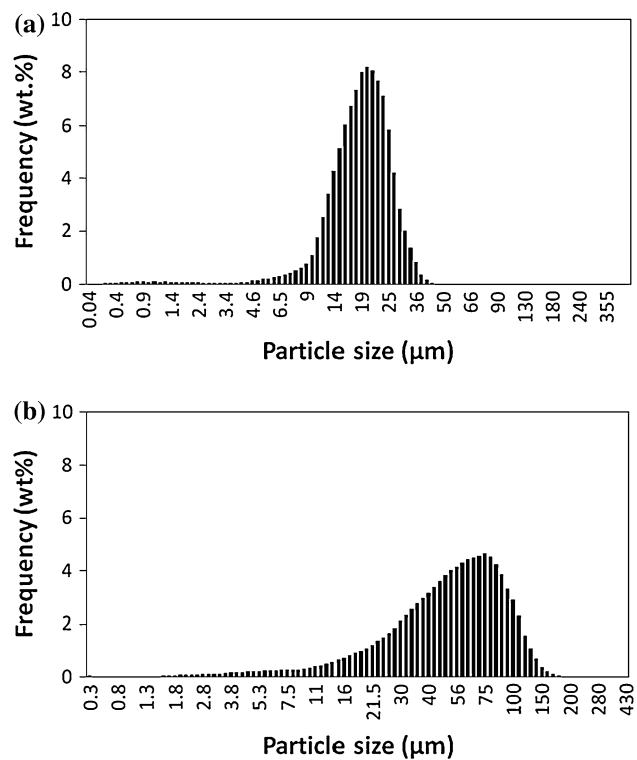


Fig. 1 The size distribution of **a** SiC and **b** Gr particles

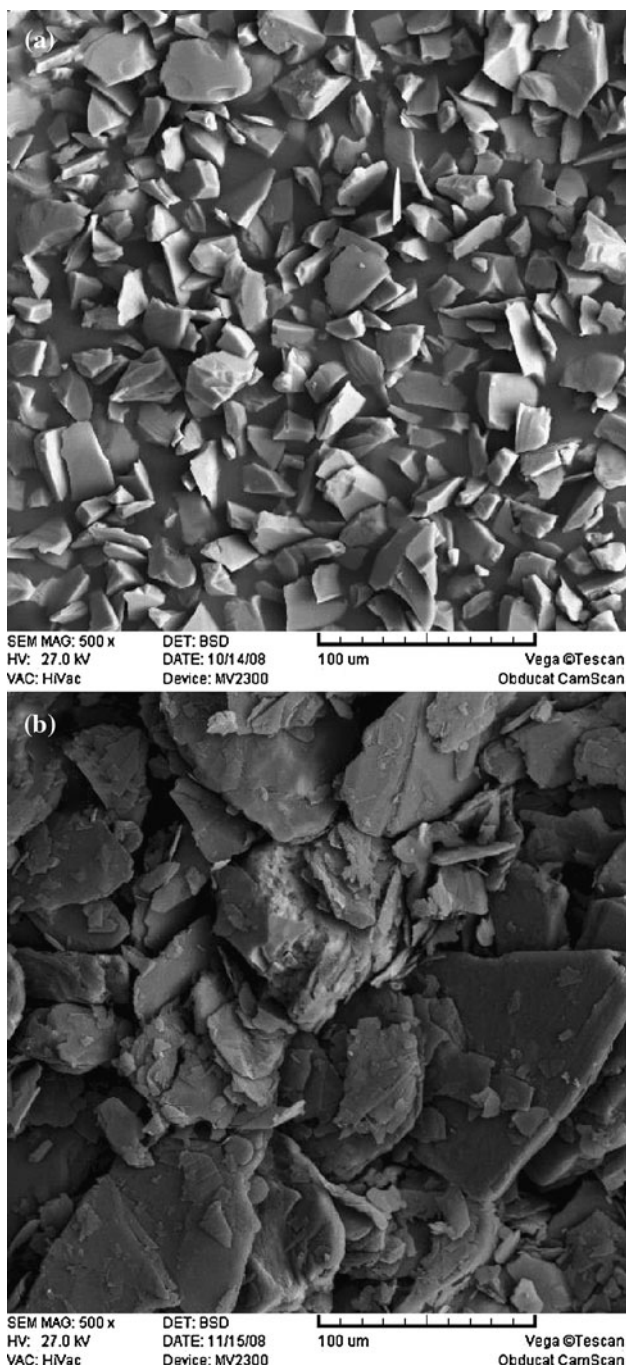


Fig. 2 SEM micrographs of **a** SiC and **b** Gr particles

Gr particles, the coarse alumina particles were sieved out from aluminum alloy–alumina powder mixtures. The resultant aluminum alloy powders were used to produce the base alloy samples. The five different batches of the powder mixtures along with the Al 6061 powders were cold pressed at six different pressures from 250 to 750 MPa in a rigid steel die on a single acting 45t hydraulic press into cylindrical compacts. The dimensions of the compacts were 25 mm in diameter and 10 mm in height. The green

compacts, which were compacted at maximum pressure (750 MPa), were sintered at 620–630 °C for 60 min in a tubular furnace and under nitrogen atmosphere to provide protection against oxidation of the aluminum matrix. In the next step, all samples were solution treated at 550 °C for 2 h prior to cold water quenching and artificially aged at 170 °C for 7 h before air cooling to room temperature.

The size distribution of the resultant powder mixtures was determined using the conventional mechanical sieving technique. Then the size distribution and the average particle size of the produced aluminum powders were calculated by considering the size distribution of the SiC and Gr powder particles. The densities of base alloy compact and the Al/Gr/SiC composites with different SiC contents were determined using Archimedes' principle in accordance with specifications in ASTM standard B-325. Hardness measurements were carried out on a Brinell hardness testing machine, using a load of 300 N. The mean values of at least five measurements conducted on different areas of each sample were considered. Pin-on-disk wear tests were done at different sliding distances of 250, 500, 750, and 1000 m. A steel pin (1.5Cr, 1C, 0.35Mn, 0.25Si) with the hardness of 64HRC having the diameter of 5 mm and height of 20 mm was employed. The imposed load and pressure on the disk were 20 N and 1 MPa, respectively. Sliding velocity in this research was 0.5 m/s. The morphology of the powder mixtures and the polished surfaces of the composites were examined using a scanning electron microscope (SEM).

Results and discussion

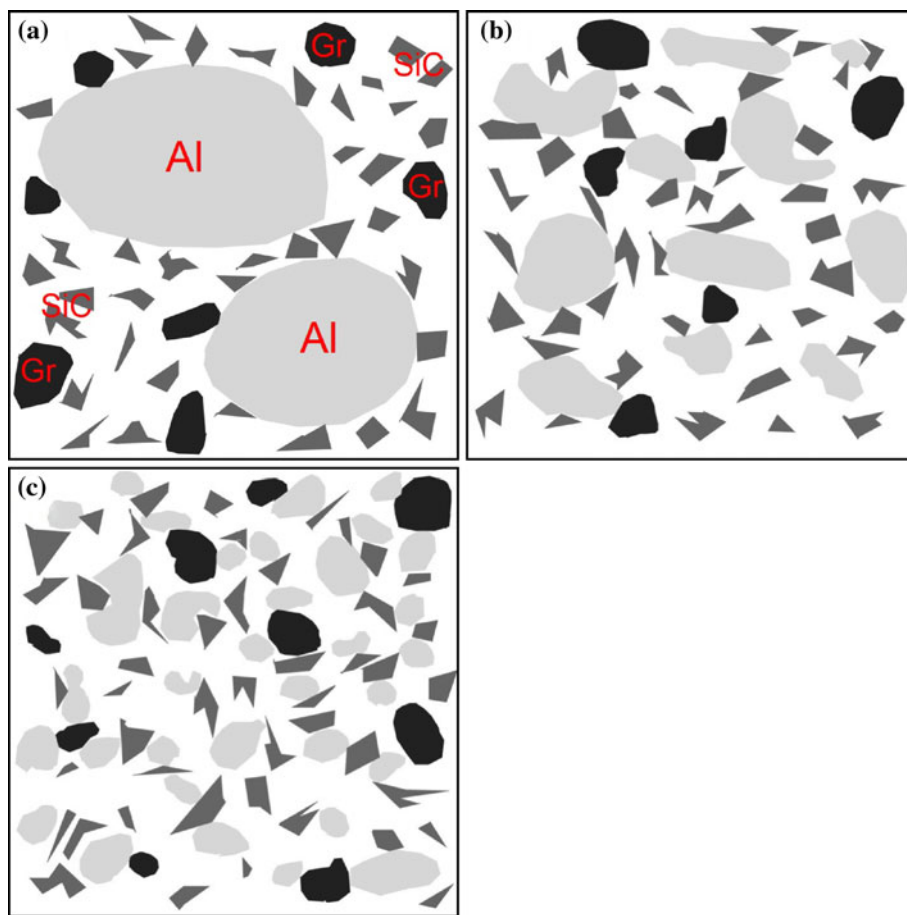
Produced powder mixtures

The SEM micrographs of the as-produced powder mixture containing 9 vol.% Gr and 40 vol.% SiC particles, within the range of <125 μm, are shown in Fig. 4. It is seen that the SiC and the Gr particles are distributed uniformly within the non-spherically shaped aluminum powders. Thus, there is no need to any additional mixing processes to obtain a uniform distribution of the reinforcing particles within the matrix alloy using IPM method. Moreover, EDX studies on the produced aluminum particles did not reveal the presence of thick aluminum oxide skins on these particles (Table 2). These results are consistent with the previous observations [24–26].

Size distribution and median size of the produced aluminum particles

Cumulative size distribution of the produced aluminum particles in the different mixtures containing 9 vol.% Gr

Fig. 3 Schematic picture of the molten aluminum fragmentation by SiC and Gr particles in the **a** initial, **b** middle, and **c** final step of the stirring process



and 0–40 vol.% SiC particles are graphically presented in Fig. 5a. The data for these plots are based on the sieve analysis of the as-produced powder mixtures and by considering the size distribution data of the used SiC and Gr particles. The figure shows that the size distribution plots shift toward the finer sizes by increasing the SiC content. Hence, the median size of the produced aluminum particles is also decreased (Fig. 5b). These results are consistent with previous observations [24–27]. In fact, the number and the surface area of the cutting elements, which cut the molten aluminum into the droplets, are increased by increasing the SiC content. Therefore, the amount of collision between the SiC particles and the molten aluminum is increased and the median size of the produced aluminum powders is decreased at the constant producing condition.

Compaction behavior

The die compaction behavior of the aluminum alloy powders and the hybrid powder mixtures containing different amounts of SiC particles are shown in Fig. 6. It can be seen that relative density is increased with a decreasing slope by increasing the applied pressure. Increasing the SiC content is also leading to a lower densification extent. These results

are consistent with the trends reported by some investigators [23, 30, 32]. The mechanisms of densification in cold compaction are rearrangement of powder particles, plastic deformation of soft particles, and fracture of hard (brittle) particles, respectively [8, 17, 22, 23, 30, 33, 34]. The rearrangement of particles and local plastic deformation are occurred at the first stages of compaction process and cause considerable increasing of the relative density. However, more displacement and rearrangement of powder particles are restricted by more plastic deformation of the aluminum particles with increasing of the compacting pressure. At this stage, the plastic deformation of the soft particles is the main process of densification, and needs the introduction of high pressures. Hence, the increasing of density is negligible at this stage.

The compressibility of aluminum matrix is decreased by increasing the SiC content in the powder mixtures. As a result, it is seen that the 40 vol.% SiC contained composite has the worst densification behavior (Fig. 6). The SiC particles are not deformable and they support a part of the applied pressure elastically. Amount of pressure is also wasted because of the friction between the SiC particles. Therefore, the transferred load to the aluminum (plastic phase) is decreased. In fact, the compressibility is reduced

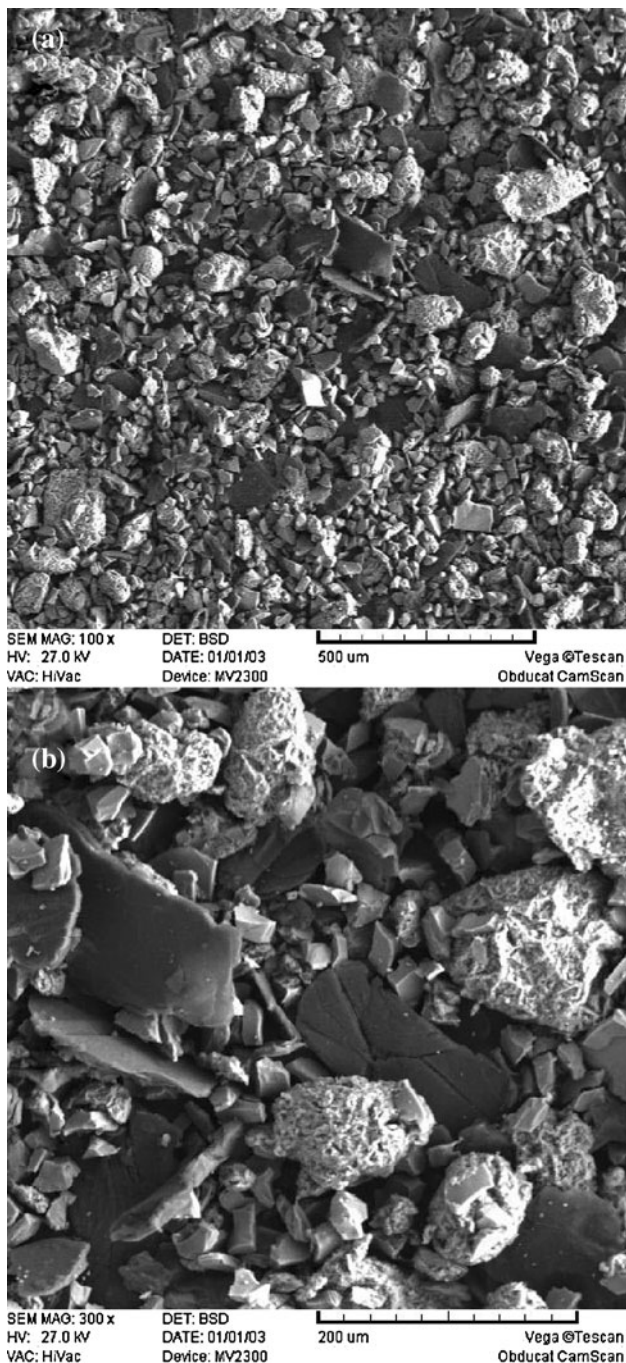


Fig. 4 Typical SEM micrographs of the as-produced powder mixture containing aluminum powders, 9 vol.% Gr and 40 vol.% of SiC particles. **a** Low-magnification micrograph, and **b** high-magnification micrograph

Table 2 EDX analytical results of the produced aluminum particles

Element	Al	Mg	O
Weight percent	98.33	0.80	0.87

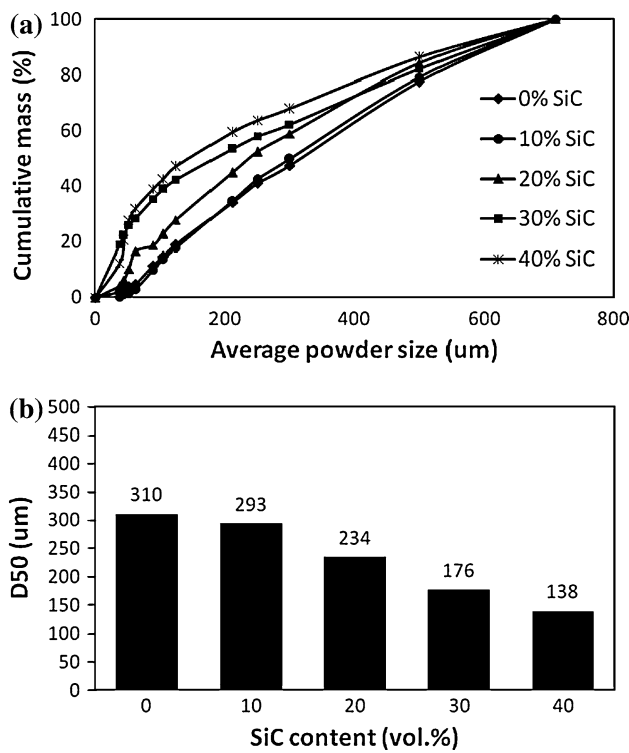


Fig. 5 Effect of SiC content in presence of 9 vol.% Gr on the size of as-produced aluminum particles with IPM method: **a** cumulative size distribution and **b** median size

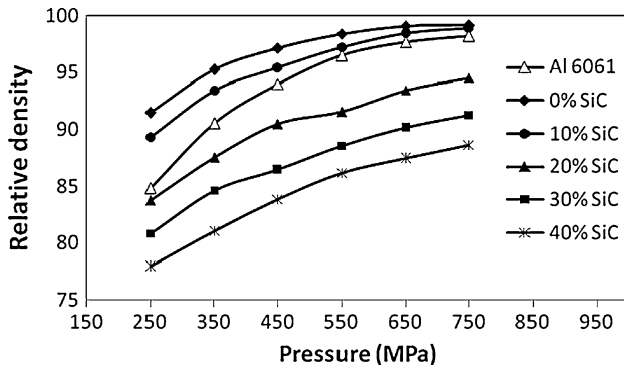


Fig. 6 Compressibility curves of different powder mixtures

by the necessity of more deformation of the aluminum particles to fill the pores at the contact points with SiC particles. Movement and rearrangement of the aluminum particles are also more limited by increasing the SiC content in the powder mixtures, and cause retarding the densification mechanism. In addition, finer aluminum particles are resulted by increasing the SiC content at the powder mixture producing stage of IPM method (Fig. 5). Finer aluminum particles in the powder mixtures are associated with a larger surface area, which in turn, increases friction between the particles and reduces the densification extent. On the other hand, finer aluminum particles imply larger

yield stresses which cause the compressibility decline. Thus, beside of direct effects of the SiC particles in reduction of the relative density, they deteriorate the densification behavior of the mixtures by decreasing the size of produced aluminum powders.

It is clear from Fig. 6 (by comparison of Al-9 vol.%Gr and Al-10 vol.%SiC-9 vol.%Gr composites with unreinforced alloy compact) that Gr, to some extent, is a compensation for destructive effects of the SiC particles in the compressibility of hybrid powder mixtures. Gr reduces the particles–die wall friction and the friction between particles, and facilitates movement and rearrangement of the aluminum powders during cold pressing. Hence, the die is better filled and higher densities are attainable.

Microstructure

The typical SEM micrographs of the polished surfaces of the Al-9 vol.%Gr composites containing 0 and 20 vol.% of SiC particles are presented in Fig. 7a–d. Figure 7 shows that the SiC and Gr particles have been distributed uniformly within the matrix alloy. This uniform distribution of the reinforcing particles is the characteristic of IPM method improving the mechanical and the tribological properties of the composites due to lack of the ceramic particle clusters. The dark regions in this pictures are the Gr particles or the pores that formed by evacuation of Gr particles during polishing the surface. Gr as a solid lubricant material is abraded easily during polishing of the hybrid composites, and therefore reduces the coefficient of friction.

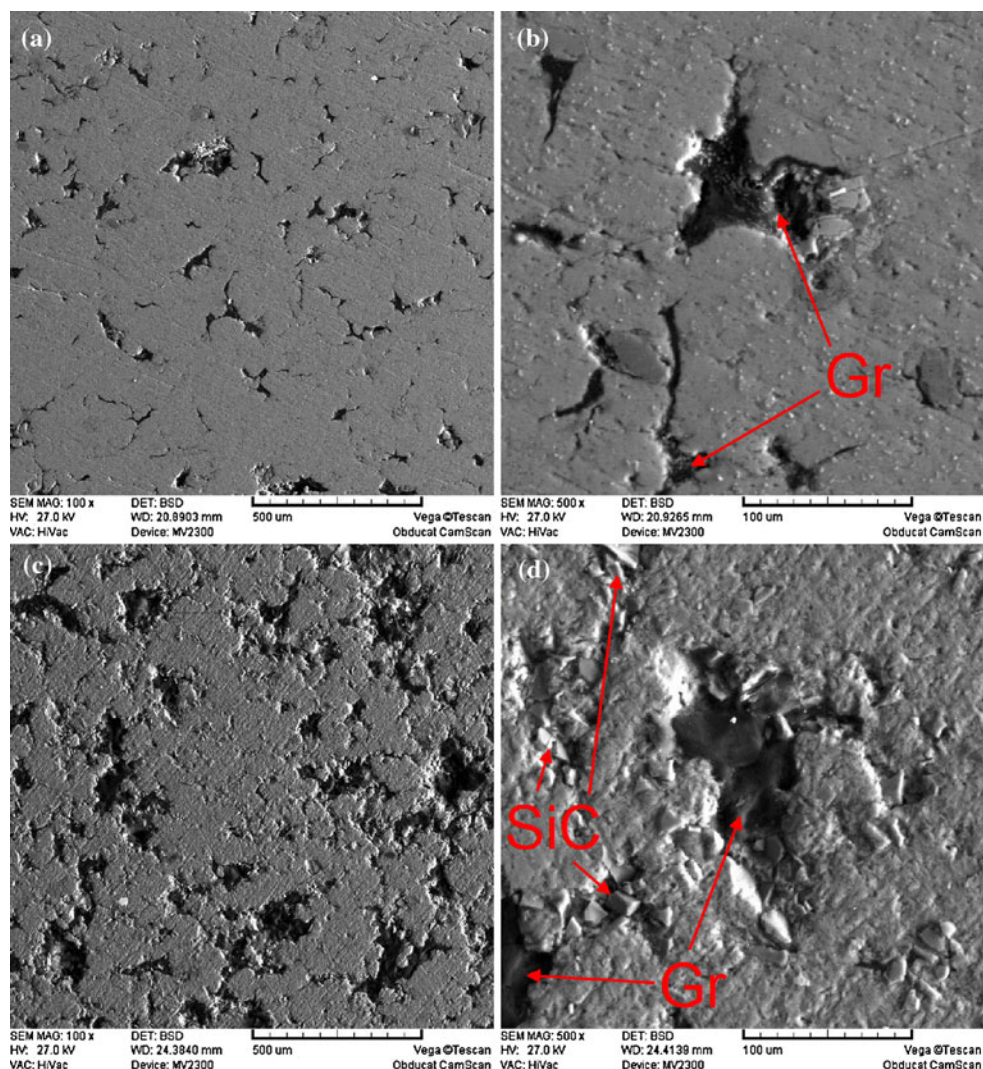


Fig. 7 Typical SEM micrographs of the polished surfaces of Al-9 vol.%Gr composites containing **a**, **b** 0 and **c**, **d** 20 vol.% of SiC particles

Porosity

The amount of porosity after sintering is a function of initial green density and it is increased by increasing the SiC content in the hybrid composites. However, it is obvious from Fig. 8 that the amount of porosity after sintering is decreased compared with the green compacts. This decline is due to the elimination of inter-particular voids and shrinkage after sintering. The same trend after sintering under nitrogen atmosphere has also been reported by other investigators [35, 36].

Hardness

Improvement in hardness with increasing the SiC content in the as sintered Al-9 vol.%Gr composites, as presented in Fig. 9, is attributable to increasing hard SiC particles in the hybrid composites. These particles also cause more deformation of the aluminum matrix and increase in dislocation density. Similar results have been reported by other investigators [10, 37–41]. The volume fraction of porosity and probability of agglomeration of the SiC particles are also increased by increasing the SiC content. However, it seems that the effects of SiC particles in hardness improvement are superior to their effects in reducing of density and decreasing of hardness values.

Gr leads to decline in hardness values. This is approved with reference to the hardness value of the 9 vol.% Gr contained composite with no SiC addition and Al 6061 sample represented in Fig. 9. Dislocation density within the matrix alloy is increased by the addition of the Gr particles, because of mismatch in coefficients of thermal expansions of Gr and aluminum alloy. Therefore, hardness value of Al-9 vol.%Gr composite should be higher than that of unreinforced alloy, but due to the soft nature of Gr, its lowering effect on hardness is more remarkable.

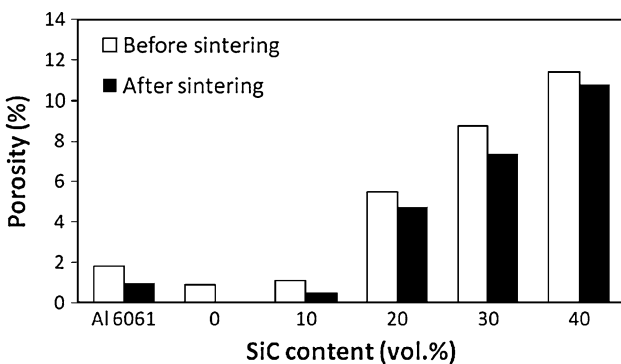


Fig. 8 Porosity variations after sintering of samples containing 9 vol.% Gr and different percents of SiC particles. The values of the Al 6061 powder compact (with no Gr addition) is also presented for comparison

Heat treatment

The strength of Al 6061 matrix composites can be improved using T6 age hardening heat treatment. Using higher amount of reinforcement content in the hybrid composites brings about a decrease in the amount of aluminum alloy (age-hardenable phase). Therefore, increase in hardness after heat treatment should be higher in the composites containing lower amounts of reinforcements. However, there is an optimum aging time for each composite sample containing different percentages of reinforcing particles. As mentioned, the mismatch of coefficients of thermal expansions in aluminum matrix and reinforcing phases causes formation of dislocation in the reinforcement–matrix interface. The higher dislocation density promotes diffusion of the alloying elements, which leads to higher nucleation and growth rate of the precipitates [40–42]. The aging kinetic is also accelerated by the possibility of heterogeneous nucleation of metastable phases on the SiC particles [41]. Thus, obviously, the aging kinetics of composite samples is faster than that of unreinforced alloy sample. Figure 10 shows the amount of increasing of hardness of the Al-9 vol.%Gr composites

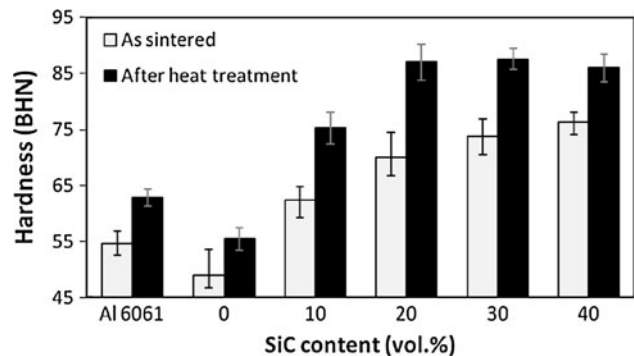


Fig. 9 The variation of hardness with SiC content for Al-9 vol.%Gr hybrid composites containing different percentages of SiC particles. The values for the matrix alloy (made from Al 6061 powders with no Gr addition) are also presented for comparison

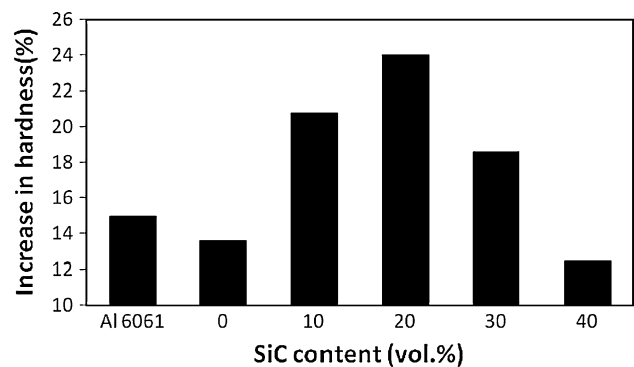


Fig. 10 Percent of increase in hardness after aging heat treatment for different samples

containing different percentages of SiC particles after aging heat treatment. The maximum increase in hardness is achieved at the Al 6061–20 vol.%SiC–9 vol.%Gr hybrid composite. Considering the same condition for aging heat treatment of the all samples, it reveals that aging time for this composite may be closer to the optimum condition (peak-aged), and in the other composites the peak hardness may not be obtained because of under-aged or over-aged conditions. Therefore, the difference between the hardness values of the hybrid composites containing 20, 30, and 40 vol.% SiC particles is reduced after aging heat treatment (Fig. 9).

Tribological behavior

Effect of the SiC content on the volume loss and the wear rate of 9 vol.% Gr contained composites and unreinforced aluminum alloy is shown in Fig. 11. It is seen that the dry sliding volume loss of all hybrid composites is lower than that of the base alloy. However, the volume loss and the wear rate of Al–9 vol.%Gr composite is higher than that of the base alloy and the hybrid composites, as reported by several researchers [12, 25, 27, 43–45]. Gr is a solid

lubricant material. It comes onto the surface resulting in the formation of a lubricating film, which prevents metal-to-metal contact of the sliding surfaces [10, 46, 47]. However, Gr is a weak phase that deteriorates the hardness and mechanical properties of composites [10, 27]. It seems that the destructive effects of 9 vol.% Gr in deterioration of mechanical and wear properties of Al–Gr composite is more than its beneficial effects in formation of lubricating film.

Figure 11 reveals that the volume loss and the wear rate of hybrid composites are decreased by increasing the SiC content to 20 vol.%, and after that any increase in SiC content leads to their increases. The wear rate of the hybrid composite containing 20 vol.% SiC particles is about eight times lower than that of the base alloy sample. These results are in line with the trends reported by other investigators [3, 4]. According to the Archard theory, wear resistance is proportional to the hardness of material [48]. Given hardness values of samples after aging heat treatment (Fig. 9), the improvement in the wear resistance of the hybrid composites resulted from increasing the SiC content to 20 vol.% can be attributed to the increasing of the hardness of the composites. However, the hardness values of the hybrid composites containing 20, 30, and 40 vol.% SiC particles are near together. In this case, the main causes of increased wear loss and wear rate with increasing of the SiC content are the increasing of porosity (Fig. 8), as well as the deterioration of particles bonding. The worn surface morphology of the hybrid composites containing 20 and 40 vol.% SiC particles is shown in Fig. 12. It is seen that the non-clear grooves and fine scratches were formed on the worn surface of both composites. The hybrid composite containing 20 vol.% SiC has a smooth worn surface, but some dimples could be seen on the worn surface of the 40 vol.% SiC contained hybrid composite. The number of weak SiC–SiC contacts and thus the possibility of debonding would be higher with increase of the SiC content to 40 vol.%.

The friction force may originate from asperity deformation, plowing, and adhesion. It may also be influenced by the wear debris entrapped between two moving surfaces [49]. The variation in coefficient of friction with SiC content is shown in Fig. 13. Sharp decline in coefficient of friction of 9 vol.% Gr contained composites compared to the base alloy shows the observable effect of the formation of Gr-rich lubricating film on the tribosurface. The figure also reveals a decrease in the coefficient of friction by any increase in the SiC content up to 30 vol.%. The Gr layer will not be an effective lubricant if the adhesion force between the aluminum surface and Gr layer be less than the interlamellar shear strength of Gr [14, 47]. Addition of the SiC particles to the Al–9 vol.%Gr composite results in improvements in strength, hardness, and so, a better

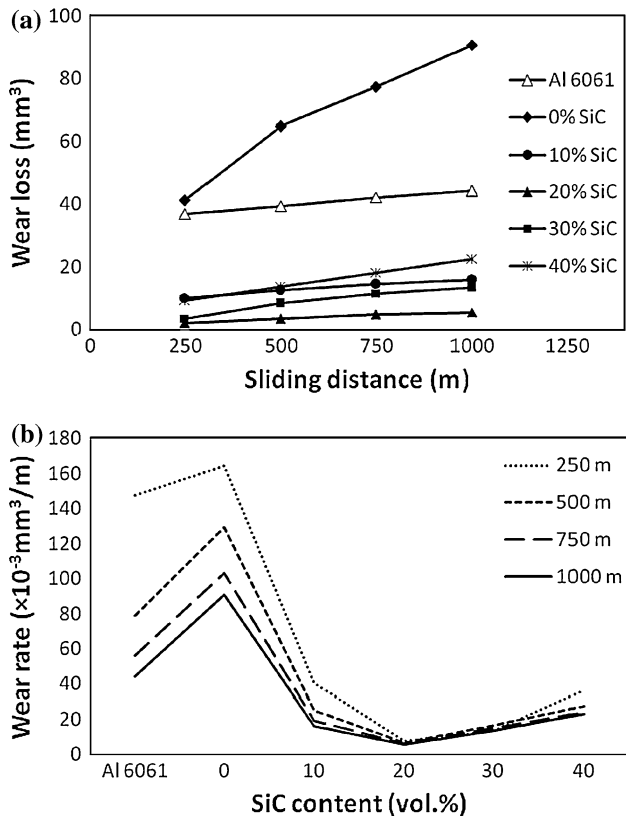


Fig. 11 The variation of **a** wear loss with sliding distance and **b** wear rate with SiC content for the hybrid composites containing 9 vol.% Gr particles

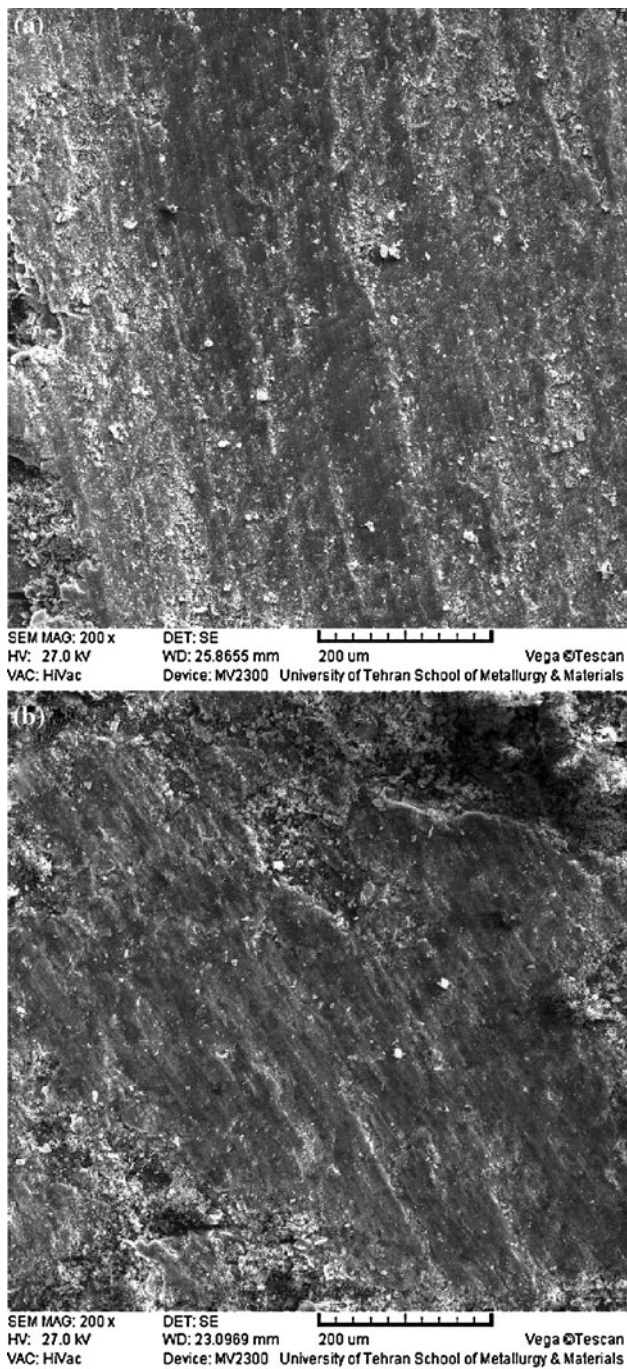


Fig. 12 Typical SEM micrographs from the worn surface of hybrid composites having **a** 20 and **b** 40 vol.% SiC content

support for the lubricating film. Increase of porosity also causes reduction in the friction coefficient [50], and the amount of porosity is increased using more SiC content in the hybrid composites (Fig. 8). However, the SiC particles removed from the matrix and entrapped between the sample and pin. This causes higher coefficient of friction of the 40 vol.% SiC contained hybrid composite.

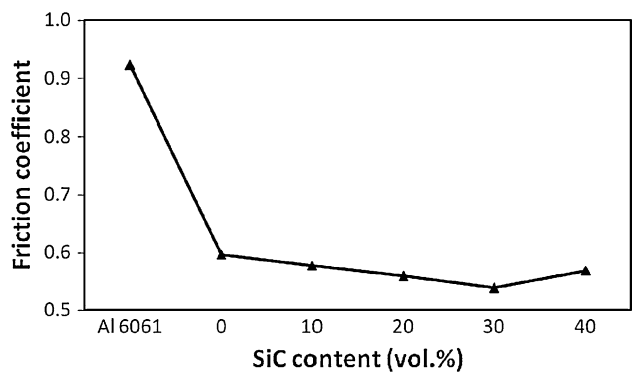


Fig. 13 The variation of friction coefficient with SiC content

Conclusions

The results of this investigation can be summarized as follows.

1. The IPM method is a new processing technique for hybrid composites which has some advantages over the conventional P/M method. In this new technique, aluminum ingot is used and no any additional mixing processes is necessary, because the production of aluminum powder particles and mixing process are done simultaneously. Therefore, it is more economical method than conventional P/M.
2. The SiC and Gr particles are distributed uniformly within the matrix alloy using this method. Finer aluminum powders are also produced by increasing the SiC content in the powder mixture producing stage.
3. The increasing of relative density is fast at the first stages of compaction process but it is retarded by continuing the cold pressing of composites at high pressures. This is due to the unavoidable plastic deformation of aluminum particles for more increasing of relative density at higher compaction pressures.
4. The compressibility of hybrid powder mixtures is decreased by increasing of the SiC content. Therefore, the worst compaction behavior is observed in the powder mixture containing 40 vol.% of SiC particles.
5. The wear resistance of the hybrid composite containing 20 vol.% SiC and 9 vol.% Gr is superior to the unreinforced alloy and the other hybrid composites. Increase in the SiC content to 20 vol.%, after a distance of 1000 m, causes decline of the volume loss and wear rate about 88%. More increasing of the SiC content from 20 to 40 vol.% causes increase in the volume loss and wear rate by 76%.
6. The friction coefficient of all composites is lower than that of the base alloy sample. The coefficient of friction is decreased by increasing of the SiC content

up to 30 vol.%, and it will be minimum at 30 vol.% SiC contained hybrid composite.

References

1. Basavarajappa S, Chandramohan G, Mukund K, Ashwin M, Prabu M (2006) *J Mater Eng Perform* 15:668
2. Ted Guo ML, Tsao CYA (2000) *Compos Sci Technol* 60:65
3. Roy D, Basu B, Mallick AB (2005) *Intermetallics* 13:733
4. Ramesh CS, Anwar-Khan AR, Ravikumar N, Savanprabhu P (2005) *Wear* 259:602
5. Lee KB, Kwon H (2002) *Metall Mater Trans A* 33A:455
6. O'Donnell G, Looney L (2001) *Mater Sci Eng A* 303:292
7. Yang G, Fan T, Zhang D (2004) *J Mater Sci* 39:3689. doi: [10.1023/B:JMSC.0000030722.14054.e2](https://doi.org/10.1023/B:JMSC.0000030722.14054.e2)
8. Ejiofor JU, Okorie BA, Reddy RG (1997) *J Mater Eng Perform* 6:326
9. Gui M, Kang SB (2001) *Metall Mater Trans A* 32A:2383
10. Suresha S, Sridhara BH (2010) *Mater Des* 31:4470
11. Leng J, Jiang L, Zhang Q, Wu G, Sun D, Zhou Q (2008) *J Mater Sci* 43:6495. doi: [10.1007/s10853-008-2974-6](https://doi.org/10.1007/s10853-008-2974-6)
12. Leng J, Jiang L, Wu G, Tian S, Chen G (2009) *Rare Met Mater Eng* 38:1894
13. Ge D, Gu M (2001) *Mater Lett* 49:334
14. Urena A, Rams J, Campo M, Sanchez M (2009) *Wear* 266:1128
15. Tien YM, Wu PL, Huang WH, Kuo MF, Chu CA (2007) *Powder Technol* 173:140
16. Nor SSM, Rahman MM, Tarlochan F, Shahida B, Ariffin AK (2008) *J Mater Process Technol* 207:118
17. Jiang G, Daehn GS, Lannutti JJ, Fu Y, Wagoner RH (2001) *Acta Mater* 49:1471
18. Huang HS, Lin YC, Hwang KS (2002) *Int J Refract Met Hard Mater* 20:175
19. Ted Guo ML, Tsao CYA (2002) *Mater Sci Eng A* 333:134
20. Akhlaghi F, Pelaseyyed SA (2004) *Mater Sci Eng A* 385:258
21. Leng J, Wu G, Zhou Q, Dou Z, Huang X (2008) *Scripta Mater* 59:619
22. Smith LN, Midha PS, Graham AD (1998) *J Mater Process Technol* 79:94
23. Hafizpour HR, Sanjari M, Simchi A (2009) *Mater Des* 30:1518
24. Mahdavi S, Akhlaghi F (2009) In: *Proceedings of the IIAC*, Tehran, pp 106–112
25. Akhlaghi F, Mahdavi S (2009) In: *Proceedings of the AMPT*, Kuala Lumpur, pp 250–257
26. Akhlaghi F, Esfandiari H (2007) *Mater Sci Technol* 23:646
27. Akhlaghi F, Zare-Bidaki A (2009) *Wear* 266:37
28. Shim Y, Levine LE, Fields RJ (2005) *Physica A* 348:1
29. Sridhar I, Fleck NA (2000) *Acta Mater* 48:3341
30. Martin CL, Lame O, Bouvard D (2000) *Mech Mater* 32:405
31. Srivatsan TS, Al-Hajri M, Petraroli M, Hotton B, Lam PC (2002) *Mater Sci Eng A* 325:202
32. Hafizpour HR, Simchi A, Parvizi S (2010) *Adv Powder Technol* 21:273
33. Al-Qureshi HA, Soares MRF, Hotza D, Alves MC, Klein AN (2008) *J Mater Process Technol* 199:417
34. Poquillon D, Lemaitre J, Baco-Carles V, Tailhades Ph, Lacaze J (2002) *Powder Technol* 126:65
35. Martin M, Castro F (2003) *J Mater Process Technol* 143–144:814
36. Showalter N, Youseff M (2008) *Mater Des* 29:752
37. Ramesh CS, Noor Ahmed R, Mujeebu MA, Abdulla MZ (2009) *Mater Des* 30:1957
38. Unlu BS (2008) *Mater Des* 29:2002
39. Zhan Y, Zhang G (2003) *J Mater Sci Lett* 22:1087
40. Parvin N, Assadifard R, Safarzadeh P, Sheibani S, Marashi P (2008) *Mater Sci Eng A* 492:134
41. Seyed Reihani SM (2006) *Mater Des* 27:216
42. Salvo L, Suery M, Towle D, Friend CM (1996) *Composites A* 27A:1201
43. Jha AK, Prasad SV, Upadhyaya GS (1989) *Tribol Int* 22:321
44. Jha AK, Prasad SV (1989) *Wear* 133:163
45. Fuentes R, Rubio E, Gomez C, Herrera A, Castano VM (2003) *Int Lubr Tribol* 55:157
46. Liu YB, Lim SC, Ray S, Rohatgi PK (1992) *Wear* 159:201
47. Prasad SV, McConnell BD (1991) *Wear* 149:241
48. Archard JF (1953) *J Appl Phys* 24:981
49. Wang L, He Y, Zhou J, Duszczyk J (2010) *Tribol Int* 43:299
50. Teoh SH, Thampuran R, Seah WKH (1998) *Wear* 214:237